water

MDPI

Article

Study on the SBA-15 Silica and ETS-10 Titanosilicate as Efficient Adsorbents for Cu(II) Removal from Aqueous Solution

Doina Humelnicu [1,*], Inga Zinicovscaia [2,3], Ionel Humelnicu [1], Maria Ignat [1], Nikita Yushin [2] and Dmitrii Grozdov [2]

[1] Faculty of Chemistry, Alexandru Ioan Cuza University of Iasi, Boulevard Carol I, 11, 700506 Iasi, Romania; ionel@uaic.ro (I.H.); maria.ignat@uaic.ro (M.I.)
[2] Joint Institute for Nuclear Research, Joliot-Curie Street, 6, 1419890 Dubna, Russia; zinikovskaia@mail.ru (I.Z.); ynik_62@mail.ru (N.Y.); dsgrozdov@rambler.ru (D.G.)
[3] Horia Hulubei National Institute for R&D in Physics and Nuclear Engineering, 30 Reactorului Street MG-6, 077125 Magurele, Romania
* Correspondence: doinah@uaic.ro

Abstract: The efficiency of Cu(II) removal from aqueous solution by two adsorbents, silica SBA-15 and titanosilicate ETS-10, was investigated. Effects of various experimental parameters such as: contact time, pH, initial copper concentration, adsorbent dosage, temperature were investigated in order to determine the maximum adsorption capacity of the adsorbents. The maximum adsorption capacity of silica SBA-15 was achieved at pH 5.0, and of titanosilicate ETS-10 at pH 6.0. The Freundlich, Langmuir, and Temkin isotherm models were applied in order to describe the equilibrium adsorption of Cu(II) by the studied adsorbents. Equilibrium data fitted well to the Langmuir model with a higher adsorption capacity of ETS-10 (172.53 $mg \cdot g^{-1}$) towards Cu(II) than SBA-15 (52.71 $mg \cdot g^{-1}$). Pseudo-first- and pseudo-second-order, Elovich, and Weber–Morris intraparticle diffusion models were used for description of the experimental kinetic data. It was found that the pseudo-first-order and pseudo-second-order kinetic models were the best applicable models to describe the adsorption kinetic data. Thermodynamic parameters that characterize the process indicated that the adsorption of Cu(II) onto the two adsorbents is spontaneous and endothermic.

Keywords: mesoporous silica SBA-15; titanosilicate ETS-10; adsorption; copper

Citation: Humelnicu, D.; Zinicovscaia, I.; Humelnicu, I.; Ignat, M.; Yushin, N.; Grozdov, D. Study on the SBA-15 Silica and ETS-10 Titanosilicate as Efficient Adsorbents for Cu(II) Removal from Aqueous Solution. *Water* **2022**, *14*, 857. https://doi.org/10.3390/w14060857

Academic Editors: Cristina Palet and Julio Bastos-Arrieta

Received: 3 February 2022
Accepted: 6 March 2022
Published: 9 March 2022

1. Introduction

The problem of environment pollution with heavy metal has become one of the serious problems, particularly in the polluted aquatic system.

The release of different pollutants into the environment has increased noticeably as a result of industrialization, and thereby lowered the quality of the environment to an alarming level. Among these pollutants, heavy metals are one of the most dangerous due to their nonbiodegradability, persistence, and toxicity.

There are many situations when low concentration of heavy metals can accumulate to toxic levels through the human food chain and the biosphere from the environment, which can disturb the biochemical processes and human health [1–5]. Heavy metals, such as lead, cadmium, mercury, copper, chromium, zinc, nickel, are used in the different fields of industry such as metal plating, electrolysis, mining, metallurgy, industry fertilizer, pesticide industry, leatherworking, and dyeing industry [2,3,6].

Among the heavy metals, copper is one of the indispensable micronutrients required by organisms at low concentrations. Copper ions play an important role in the enzyme's synthesis, development of tissues and bones for human [7]. At high concentrations, copper toxicity may be observed by a variety of syndromes and effects including renal dysfunction, hypertension, hepatic injury, lung damage and teratogenic effects [8,9].

Due to the mobility and toxicity, the presence of Cu(II) ions in surface water and groundwater represents a real inorganic contamination problem. This ion is one of the most poisonous, whose toxicity is attributed in part to its ability to accumulate in tissues. Human exposure to a high level of copper results in generation of reactive oxygen species (ROS) and free radicals by Fenton-like reaction. These radical species can alter biomolecules like DNA, proteins and lipids.

Therefore, it is important to remove copper from effluents, before discharging them into water bodies. There are various common methods available for the removal of copper ions from wastewaters such as chemical precipitation [10], absorption [11,12] and biosorption [13], membrane separation [14], bioelectrochemical systems [15], ion exchange [16], and electrochemical methods [17]. However, these techniques have limitations such as low efficiency at low metal concentrations or production of secondary sludge, which furthers disposal in a costly process [18].

Among the abovementioned methods, adsorption has been regarded as a cost-effective technology for removal of heavy metals from solutions with low metal concentrations. The main advantages of the technique are low cost of adsorbents, easy desorption, good recycling, highly effective and environmental-friendly nature [1,2,5,6].

The World Health Organization (WHO) recommends a safe amount of Cu(II) of 5 mg/L in drinking water [19]. Therefore, more attention is paid to efficient methods of copper removal from residual waters.

Among the adsorbents used in the literature for the remediation of the wastewaters contaminated with copper are: zeolite [20], chitosan [21], clays [22], graphene nanocomposite [23], carbon nanotubes [24].

One of the adsorbents that is investigated in this study is an ion exchanger belonging to the Engelhard Titanium Silicate (ETS) family. The ETS-10 phase is an extremely interesting titanosilicate microporous material due to its high thermal stability and wide pores (pore size close to 0.8 nm). These materials are useful and can be applied in a variety of fields, such as water purification and heavy metal removal [25,26], gas adsorption [27], and photo-catalysis [28].

The second adsorbent that is used in this research is SBA-type silicas (Santa Barbara Amorphous) that exhibit interesting textural properties, such as large specific surface areas and uniform-sized pores. The advantage of the use of SBA-15 material includes its high surface-to-volume ratio, flexible framework compositions and high thermal stability [29].

An essential condition for an advantageous sorption is an adequately selective sorbent with a high sorption capacity and high level of reusability.

The objectives of the present study were: (i) the investigation of the influence of pH, sorbent dose, copper concentration and temperature on the sorption capacity and removal efficiency in non-competitive conditions; (ii) to model the kinetic and equilibrium of copper adsorption in order to evaluate the kinetic and isotherm parameters; (iii) to establish the level of reusability of the sorbents during consecutive sorption/desorption cycles.

The influence of initial pH of Cu(II) ions solution, contact time, adsorbent dosage and initial concentrations on the Cu(II) ions uptake was studied. The non-linear Langmuir, Freundlich and Temkin isotherm models were used to fit the equilibrium adsorption data. The adsorption rates were determined quantitatively and compared by the pseudo-first-order, pseudo-second-order, Elovich and Weber–Morris intraparticle diffusion models.

2. Materials and Methods

The sorbents have been synthesized by a sol–gel method as described in our previous work [30]. Mesoporous silica SBA-15 was synthesized in acidic conditions using amphiphilic triblock copolymer poly(ethylene glycol)-block-poly(propyleneglycol)-block-poly(ethylene glycol) (Pluronic P123—$EO_{20}PO_{70}EO_{20}$; Sigma-Aldrich, St. Louis, MO, USA) as a surfactant template and TEOS (tetraethyl orthosilicate, Sigma-Aldrich) as silica source. Titanosilicate ETS-10 with the composition $3.4Na_2O{:}1.5K_2O{:}TiO_2{:}5.5SiO_2{:}150H_2O$

has been prepared from sodium silicate (Sigma-Aldrich) as Si precursor and commercial TiO_2 (Degusa-P25, Sigma-Aldrich) as Ti source.

Sorption Experiments

All chemicals were of analytical reagent grade and no further purification was carried out.

The adsorption experiments were performed in a batch system by stirring at 200 rpm a suspension that contained Cu(II) ions solution and corresponding amounts of the adsorbent. The stock solution containing Cu(II) was prepared from $CuSO_4 \cdot 5H_2O$ (Sigma-Aldrich) and diluted to obtain the appropriate concentrations. The pH varied between 2 and 6, the initial concentration of copper in the solution ranged from 10 to 200 $mg \cdot L^{-1}$, at a temperature between 20 °C and 50 °C. The pH of the solution was adjusted with NaOH or HNO_3 0.1 M solution and measured with a HANNA pH/temperature meter HI 991001. About 0.02 g of adsorbent was added into the solution containing Cu(II) ions and was left stirring for a certain period of time. At the end of adsorption experiment, the adsorbents were separated from the solutions using cellulose nitrate membrane filters (0.45 μm pore). The concentrations of Cu(II) ions in the filtrate (before and after adsorption of Cu(II)) were determined using ICP-AES (Analytik Jena, Jena, Germany).

The Cu(II) adsorption q was calculated using the following equation:

$$q = \frac{(C_0 - C_e) \cdot V}{m} \quad (1)$$

and adsorption removal efficiency, R (%) from the equation:

$$RE = \frac{C_0 - C_e}{C_0} \cdot 100 \quad (2)$$

where q is the amount of copper ions adsorbed on the adsorbent, mg/g; V is the volume of solution, L; C_0 is the initial concentration of copper in mg/L, C_e is the final copper concentration in the solution, mg/L, and m is the mass of adsorbent, g.

The adsorption capacities of the two adsorbents were analyzed through the use of the Langmuir, Freundlich and Temkin isotherm models. The kinetics of copper adsorption on the ETS-10 and SBA-15 were analyzed using pseudo-first-order, pseudo-second-order, Elovich and Weber–Morris intra-particle diffusion kinetic models.

All batch adsorption experiments were carried out in duplicate and results are presented as arithmetic mean values.

3. Results and Discussion

The adsorbents were characterized by DRX, FT-IR, thermal analysis and SEM-EDX, as we have reported in our previous work [30]. The obtained results indicated that the adsorbents are mesoporous material with a BET surface area of 802.493 s/g for silica SBA-15, and microporous material with a surface area of 31.473 s/g for titanosilicate ETS-10, respectively.

3.1. pH Effect on the Adsorption Process

The adsorption of Cu(II) ions onto the adsorbents varies depending on initial pH, because this parameter causes changes in the charge of adsorbent, the degree of ionization and speciation of the adsorbate.

In this study, the range of initial pH for Cu(II) ions adsorption study was 2.0–6.0. At pH values higher than 7, precipitation of Cu(II) ions as $Cu(OH)_2$ occurs and could lead to the wrong interpretation of adsorption data. On Figure 1 is shown the removal efficiency of the SBA-15 and ETS-10 for Cu(II) ions. As can be seen from Figure 1, the sorption capacity of Cu(II) ions onto the adsorbents increased with an increase in the initial pH value of the solution. The maximum sorption of Cu(II) ions onto adsorbents occurred at pH 6 for ETS-10 and pH 5 for SBA-15, respectively. It was observed that a sharp increase in the copper removal from 8.6% to 99.61% (SBA-15) and from 10% to 99.79% (ETS-10) occurred when

the pH values of the solutions changed from 2.0 to 6.0. The low removal efficiency at low pH is apparently due to the presence of a higher concentration of $[H_3O]^+$ in the solution which competes strongly with the Cu(II) ions for the adsorption sites of the SBA-15 and ETS-10 surfaces. With the pH increase, the $[H_3O]^+$ concentration decreases leading to an increase of Cu(II) uptake.

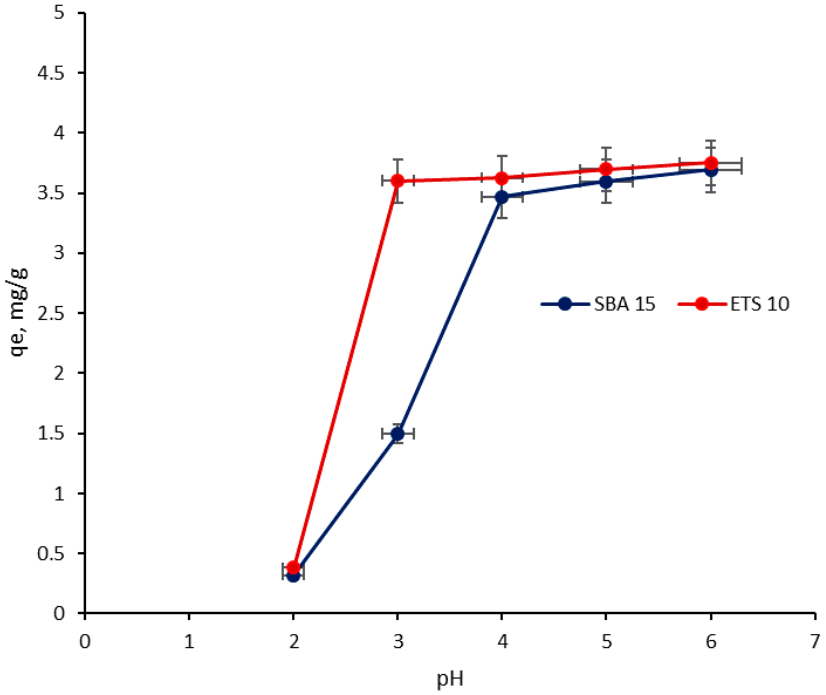

Figure 1. pH influence on the removal efficiency of SBA-15 and ETS-10 adsorbents toward Cu(II). (Ci 10 mg/L, time 60 min, temperature 23 °C, adsorbent dose 20 mg).

3.2. Effect of Adsorbent Dosage

An important parameter that affects the efficiency of adsorption from an economic point of view is the mass of the sorbent. The adsorption process is not effective if it requires a large amount of adsorbent. The influence of the adsorbent mass used on the adsorption of Cu(II) ions was investigated, and the results are shown in Figure 2. The doses of adsorbents varied from 0.010 g to 0.050 g, while the other parameters such as pH, temperature, initial concentration of Cu(II) ions, contact time were kept constant. Based on Figure 2, it is seen that an increase of the adsorbent dose can lead to an increase in the percentage of Cu(II) ions removal from the solution. This is anticipated because, by increasing the adsorbent's dose, the number of adsorption sites available for adsorbent–adsorbate interaction will increase as well. Both adsorbents showed no further increase in the adsorption capacity after a certain amount of adsorbent was added.

3.3. Equilibrium Isotherm, Kinetics and Thermodynamic Studies

3.3.1. Adsorption Equilibrium Isotherm

Adsorption isotherms are fundamental for understanding the mechanism of adsorption and the interaction between sorbent and sorbate. To study the adsorption of Cu(II) onto the sorbent, three of the most commonly used isotherm models were used in this work: Langmuir, Freundlich and Temkin. The Langmuir [31] (Equation (3)) isotherm model characterizes an adsorption monolayer on a surface with a finite number of identical centers that are homogeneously distributed on the surface of sorbent. This model assumes that the binding sites are homogeneously distributed over the adsorbent surface and the binding sites have the same affinity for adsorption of a single molecular layer. The bonding to the

adsorption sites can be either chemical or physical in nature, but must be strong enough to avoid displacement of the adsorbed Cu(II) ions.

$$q_e = \frac{q_m \cdot K_L \cdot C_e}{1 + K_L C_e} \quad (3)$$

where q_e is the amount of Cu(II) adsorbed per mass unit of sorbent at equilibrium ($mg \cdot g^{-1}$), C_e is the equilibrium concentration of remaining Cu(II) ions in the solution ($mg \cdot L^{-1}$), q_m is a parameter that gives the maximum adsorption capacity of the sorbent ($mg \cdot g^{-1}$), K_L is a constant that refers to the energy of adsorption/desorption ($L \cdot mg^{-1}$).

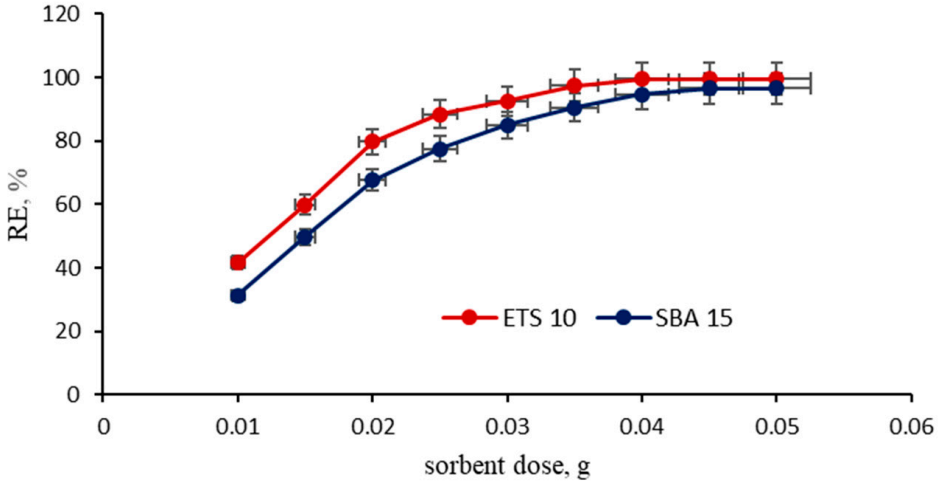

Figure 2. Influence of adsorbent dose on the removal efficiency of SBA-15 and ETS-10 adsorbents toward Cu(II). (C_i 10 mg/L, time 60 min, temperature 23 °C).

The Freundlich [32] (Equation (4)) isotherm is the second mathematical model used to describe the adsorption metal present in solution on solid surface. This model assumes that the adsorbent has an energetically heterogeneous surface and has a different affinity for adsorption.

$$q_e = K_F \cdot C_e^{1/n} \quad (4)$$

where q_e is the amount of Cu(II) adsorbed at equilibrium ($mg \cdot g^{-1}$); C_e is the concentration of Cu(II) ion in solution at equilibrium ($mg \cdot L^{-1}$); K_F ($L \cdot mg^{-1}$) and 1/n are the Freundlich constants.

The Temkin isotherm model [33] (Equation (5)) assumes that the adsorption heat of molecules decreases linearly with the increase in coverage of the adsorbent surface, and that adsorption is characterized by a uniform distribution of binding energies.

$$q_e = \frac{RT}{b_T} \cdot \ln(a_T \cdot C_e) \quad (5)$$

where $1/b_T$ represents the sorption potential of the sorbent, a_T is the Temkin constant, R is the universal gas constant (8.314 J $K^{-1} \cdot mol^{-1}$) and T is the temperature (K).

The interaction of metal ions and adsorbents was further evaluated by the separation factor (R_L). R_L is a dimensionless constant separation factor, an equilibrium parameter derived from the Langmuir isotherm model. The R_L was defined by Hall et al. [34], and is expressed as Equation (6).

$$R_L = \frac{1}{1 + K_L \cdot C_0} \quad (6)$$

K_L is the Langmuir constant and C_0 is the initial concentration of Cu(II) ions. For a favorable adsorption, the R_L value must be between 0 and 1. In this respect, if $R_L > 1$ adsorption is unfavorable, and if $R_L = 0$ adsorption is irreversible. In the present studies,

the obtained R_L values were less than one (Table 1), which indicated that the adsorption processes were favorable.

Table 1. Langmuir, Freundlich and Temkin isotherm parameters for the sorption of Cu(II) on silica SBA-15 and titanosilicate ETS-10 adsorbents.

Model	Parameters	Silica SBA-15	Titanosilicate ETS-10
Langmuir	q_m, mg/g	52.71	172.53
	K_L, L/mg	2.04	8.73
	R_L	0.002–0.046	0.0005–0.011
	R^2	0.984	0.999
Freundlich	K_F, mg/g	0.197	0.460
	1/n	0.95	0.86
	R^2	0.977	0.985
Temkin	a_T, L/g	0.066	0.65
	b_T, kJ/mol	0.0118	0.089
	R^2	0.735	0.833

The graphical representation of used models among with experimental data is presented in Figure 3, and the obtained values for Langmuir, Freundlich and Temkin isotherm constants and correlation coefficients are listed in Table 1.

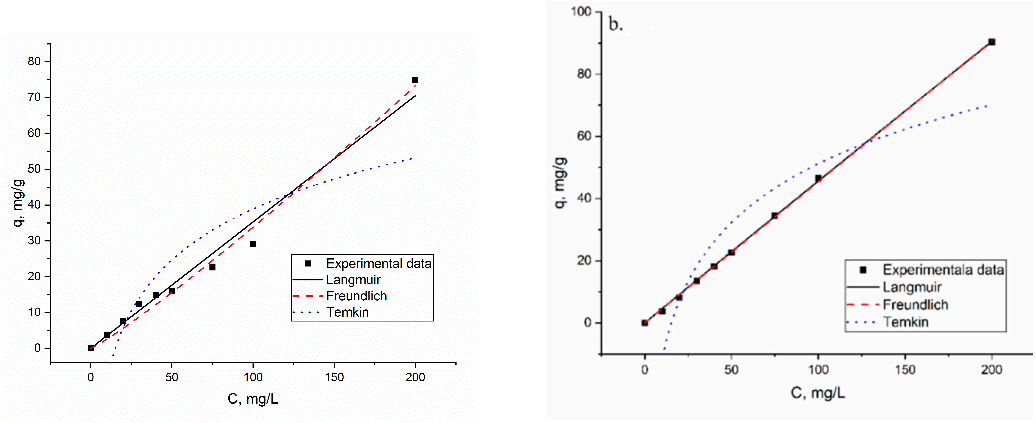

(**a**) (**b**)

Figure 3. The adsorption isotherms and experimental data for Cu(II) ion sorption on: (**a**) mesoporous silica SBA-15 and (**b**) titanosilicate ETS-10 adsorbents.

The RL values, greater than zero and lower than unit, indicate that the sorption of Cu(II) ions on both adsorbents was favorable and reversible. Sorption of Cu(II) onto SBA-15 and ETS-10 was better described by the Langmuir and Freundlich models according to the high values of R^2 for both adsorbents.

In addition, between two tested adsorbents, in terms of adsorption capacity, the best candidate seems to be ETS-10. The maximum adsorption capacity given by the Langmuir isotherm was 52.71 mg/g for SBA-15 and 172.53 mg/g for ETS-10, respectively.

Monolayer coverage of the surface by the metal ions can be used for the calculation of the specific surface area S according to the following equation [3,35]:

$$S = \frac{q_{max} \cdot N \cdot A}{M} \quad (7)$$

where S is the specific surface area, m^2/g adsorbent; q_{max} the monolayer sorption capacity, g Cu/g adsorbent; N the Avogadro number, $6.023 \cdot 10^{23}$; A the cross-sectional area of metal

ion, m^2; M the molecular weight of metal. The molecular weight and the cross-sectional area of Cu(II) are 63.5 and 1.58 $Å^2$ in a close packed monolayer (Cu(II) radius is 0.71 Å), respectively [35,36]. The maximum specific surface area calculated from Equation (7) for Cu(II) adsorption is 7.89 m^2/g for SBA-15, and 25.86 m^2/g for ETS-10, respectively. Comparison of the maximum specific surface area of the adsorbents for Cu(II) adsorption shows that SBA-15 and ETS-10 have a larger specific surface area than other adsorbents [35–37].

The efficiency of the two investigated adsorbents, ETS-10 and SBA-15, for removal of Cu(II) was highlighted by comparison with the values of maximum adsorption capacity presented in the literature for other adsorbents along with testing conditions (Table 2).

Table 2. The comparison of maximum sorption capacity of Cu(II) ions onto different adsorbents.

Adsorbent	Conditions	q, mg/g	Reference
Mesoporous silica SBA-15	pH = 5, t = 23 °C	52.71	Present study
Titanosilicate ETS-10	pH = 5, t = 23 °C	172.53	Present study
Rape straw powders	pH = 4.77, t = 20 °C	34.29	[38]
Sunflower hulls	pH = 5, t = 20 °C	49.74	[39]
Chitosan based ion-imprinted cryo-composites	pH = 4.5	260	[40]
Chemical modified Moringa oleifera leaves powder	pH = 6, t = 50 °C	167.9	[41]
Coconut tree sawdust	pH = 6	3.89	[42]
Eggshell	pH = 6	34.48	[43]
Sugarcane bagasse	pH = 6	3.65	[42]
N-HAP/Chitosan	pH = 7.5, t = 25 °C	113.66	[43]
Chitosan crosslinked with epichlorohydrin-triphosphate	pH = 6, t = 25 °C	130.38	[44]

As can be seen, the highest sorption capacities were reported for some adsorbents, such as: chitosan-based ion-imprinted cryo-composites [40], ETS-10 (present study), chemically modified moringa oleifera [41], natural hydroxyapatite/chitosan composite [43], and chitosan crosslinked with epichlorohydrin-triphosphate [44], respectively.

3.3.2. Adsorption Kinetics

In order to investigate the mechanism of adsorption, the pseudo-first-order (PFO), pseudo-second-order (PSO), Elovich and Weber–Morris models were used to study the experimental data obtained.

The pseudo-first-order model of Lagergren [45] is commonly used for the adsorption of liquid/solid systems and assumes that the rate of variation of surface site concentration is proportional to the amount of surface sites remaining unoccupied.

$$q_t = q_e(1 - e^{-k_1 t}) \quad (8)$$

where q_e and q_t are the amounts of Cu(II) ions adsorbed onto sorbents ($mg \cdot g^{-1}$) at equilibrium and at time t, respectively, and k_1 is the rate constant of first-order adsorption (min^{-1}).

The pseudo-second-order model can be expressed as [46]:

$$q_t = \frac{k_2 \cdot q_e^2 \cdot t}{1 + q_e \cdot k_2 t} \quad (9)$$

where k_2 is the rate constant of second-order adsorption ($g \cdot mg^{-1} \cdot min^{-1}$). This model is more likely to predict the adsorption behavior over the whole range of adsorption. The pseudo-second-order equation assumes that the adsorption behavior was controlled by the rate-controlling step, which can be chemical sorption involving an electronic exchange or

distribution between adsorbent and adsorbate. The adsorbate can be transferred from the solution phase to the surface of the adsorbent in several steps. The steps may include film or external diffusion (transfer of adsorbate), pore diffusion, surface diffusion and adsorption on the pore surface. The overall adsorption can occur through one or more steps. The Weber–Morris intraparticle diffusion equation is given by the following equation [47]:

$$q = k_{diff} \cdot t^{0.5} + C_i \quad (10)$$

where k_{diff} is a rate parameter ($mg/g \cdot min^{1/2}$), and C_i is the intercept, which relates to the thickness of the boundary layer

The Elovich kinetic model helps to predict the mass and surface diffusion, activation and deactivation energy of a system [48].

$$q_t = \frac{1}{\beta} \ln(1 + \alpha \cdot \beta \cdot t) \quad (11)$$

where q_t is the sorption capacity at time t (mg/g), α is the initial sorption rate ($mg \cdot g^{-1} \cdot min^{-1}$), β is the desorption constant ($g \cdot mg^{-1}$).

The graphical representation of kinetic models is presented in Figure 4, and the kinetic model constants, along with the correlation coefficient, are given in Table 3.

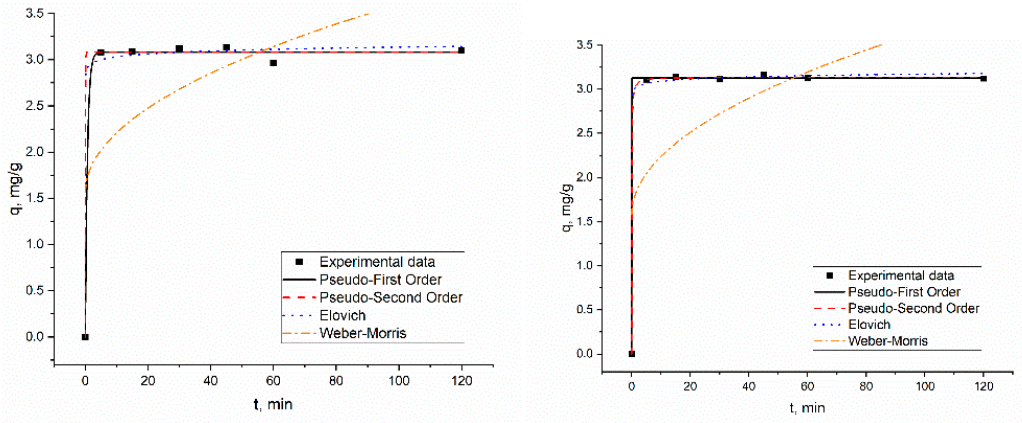

Figure 4. Kinetics of Cu(II) sorption on (**a**) mesoporous silica SBA-15 and (**b**) titanosilicate ETS-10 adsorbents.

Kinetic profiles indicated that the Cu(II) adsorption process was fast for both adsorbents. The adsorbents showed the same behavior regarding the removal of Cu (II), increasing up to 10 min and then were kept almost constant. In other words, the copper adsorption process occurred in two stages: an initial fast stage up to 10 min followed by a second stage in which no significant variation on the adsorption capacity was observed. This observation is due probably to the fact that more adsorption sites are available at the beginning of the experiments, followed by a saturation of the metal on the surface of the adsorbent.

The agreement between experimental data and the model predicted values was expressed by the correlation coefficients (R^2). A relatively high correlation coefficients value indicates that the model successfully describes the kinetics of copper adsorption. The values of R^2, both for PFO and PSO kinetic modes, are comparable, and for both models the theoretically calculated and experimentally obtained values of adsorption capacity were in good agreement. Similar results were found for other adsorbents [5,11,23]. The pseudo-second-order model assumes that the adsorption of adsorbate onto adsorbent supports second-order chemisorptions. The adsorption of copper onto SBA-15 and ETS-10

probably occurred by surface complexation reactions between copper and the sorption sites on the adsorbents.

Table 3. Parameters of the applied kinetic models for the adsorption of Cu(II) on SBA-15 and ETS-10.

	Parameter	Silica SBA-15	Titanosilicate ETS-10
	q_{exp}, mg/g	3.13	3.16
PFO	$q_{e,cal}$, mg/g	3.08	3.13
	k_1, min^{-1}	1.463	194.67
	R^2	0.997	0.999
PSO	$q_{e,\,cal}$, mg/g	3.081	3.135
	k_2, g/mg·min	$2.87 \cdot 10^{44}$	7.321
	R^2	0.997	0.999
Elovich	α, mg/g·min	$6.29 \cdot 10^{26}$	$7.08 \cdot 10^{34}$
	β, g/min	22.133	27.81
	R^2	0.994	0.998
Weber–Morris	k_{diff}	0.204	0.208
	C_i	1.565	1.577
	R^2	0.284	0.295

3.3.3. Thermodynamic Parameters

The thermodynamic parameters could be used to conclude whether the sorption process was spontaneous or not in the behavior of SBA-15 and ETS-10 sorbents for removal of Cu(II).

As reported by Guo et al. [49] and Kumar et al. [50], the values of the distribution coefficient (K_d), calculated using Equation (12) at different temperatures of 20 °C, 30 °C, 40 °C and 50 °C, were used to evaluate the thermodynamic parameters (ΔG°, ΔH°, and ΔS°).

$$K_d = \frac{q_e}{C_e} \cdot M_{adsorbate} \quad (12)$$

where q_e is the amount of Cu(II) retained at equilibrium, $mg \cdot g^{-1}$, C_e is the concentration of Cu(II) at equilibrium, in the aqueous phase, $mg \cdot L^{-1}$, and $M_{adsorbate}$ is the mass of Cu(II).

In order to solve the problem of the dimensionless of K_d, the values were multiplied with 55.5 $mol \cdot L^{-1}$ [51], the obtained value being symbolized with K°.

Equation van't Hoff (13) was used for calculation of enthalpy and entropy from the slope and intercept of plot lnK° vs. 1/T (Figure 5).

$$\ln K^0 = \frac{\Delta S^0}{R} - \frac{\Delta H^0}{RT} \quad (13)$$

where R is the universal gas constant (8.314 $J \cdot mol^{-1} \cdot K^{-1}$), T is the absolute temperature (K).

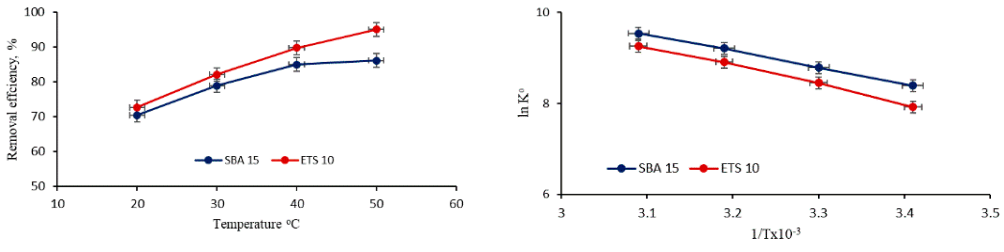

(**a**) (**b**)

Figure 5. Temperature dependence (**a**) of removal efficiency of Cu(II) onto SBA-15 and ETS-10 sorbents and plot for the evaluation of the thermodynamic parameters (**b**).

The standard Gibbs free energy change can be calculated by the following equation:

$$\Delta G^0 = -RT \ln K^0 \quad (14)$$

The obtained results are presented in Table 4.

Table 4. Thermodynamic parameters of the sorption process.

Sorbent	ΔH^0, kJ/mol	ΔS^0, kJ/mol·K	ΔG^0, kJ/mol			
			293	303	313	323
SBA-15	30.09	0.172	−20.31	−22.03	−23.75	−25.47
ETS-10	34.86	0.185	−19.35	−21.19	−23.05	−24.89

The positive values of ΔH^0 (ETS-10 = 34.86 kJ/mol, SBA-15 = 30.09 kJ/mol) denoted that the sorption process was of endothermic nature. The positive values of ΔS^0 (ETS-10 = 0.185 kJ/mol·K, SBA-15 = 0.172 kJ/mol·K) indicate increasing in randomness at the solid–liquid interface or changing the original internal structure of absorbent during the sorption process in Cu(II) aqueous solution. The increase of the negative value of ΔG^0 with the increase of temperature supports the increase of the degree of spontaneity for the sorption of Cu(II) onto both adsorbents.

Thermodynamic parameters revealed that sorption behavior was spontaneous and chemical in nature (almost all values of $\Delta G^0 > -20$ kJ·mol^{-1}) in the process of adsorption of Cu(II) using ETS-10 and SBA-15 as sorbents.

The activation energy of the sorption process (E_a) was obtained from the slope of plotting $\ln(1 - \theta)$ vs. $1/T$, where sorbent surface coverage (θ) was calculated using Equation (15) [52]:

$$\theta = \left(1 - \frac{C_e}{C_0}\right) \quad (15)$$

C_e, C_0 are equilibrium and initial concentration of Cu(II) in aqueous solution (mg/L).

According to the modified Arrhenius equation, plotting $\ln(1 - \theta)$ vs. $1/T$ (Figure 6) gives a straight line with the slope E_a/R.

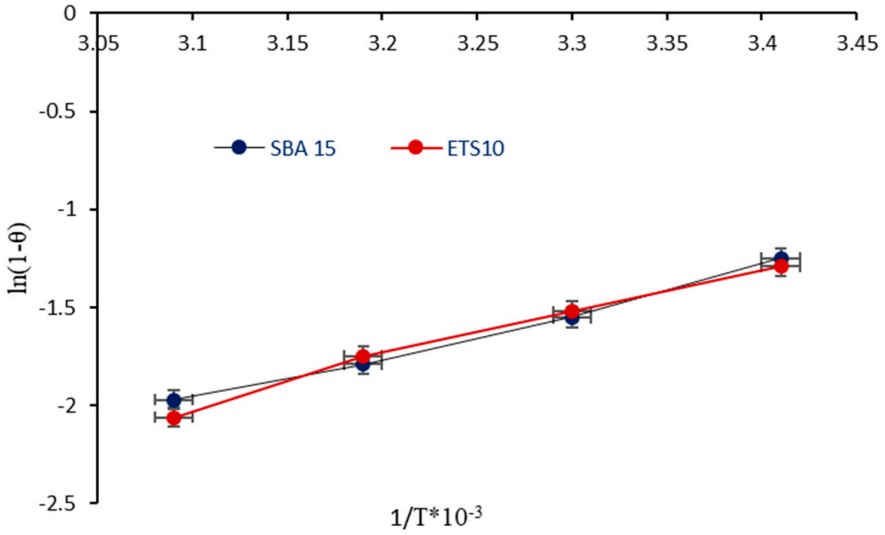

Figure 6. Plot of ln(1-θ) vs. 1/T.

Activation energy values are calculated from the slope of plot and were found to be 43.54 kJ·mol^{-1} and 18.18 kJ·mol^{-1} for ETS-10 and SBA 15, respectively. The positive values of E_a were consistent with the obtained positive values of ΔH° and confirm once more the endothermic nature of the sorption process.

3.4. Modelling of the Interactions

The interactions between the structures of mesoporous silicas SBA-15 and microporous titanosilicate ETS-10 with $CuSO_4 \cdot 5H_2O$ were simulated using the theoretical chemistry methods. The adsorbent macrostructures were represented, in gaseous medium, by a small fragment that respects the atomic arrangement according to the crystalline structures from the Crystallography Open Database (COD). For the sulfate molecule was used a structure with an octahedral configuration for the Cu atom, illustrated in Figure 7a, similar with the one representation in COD.

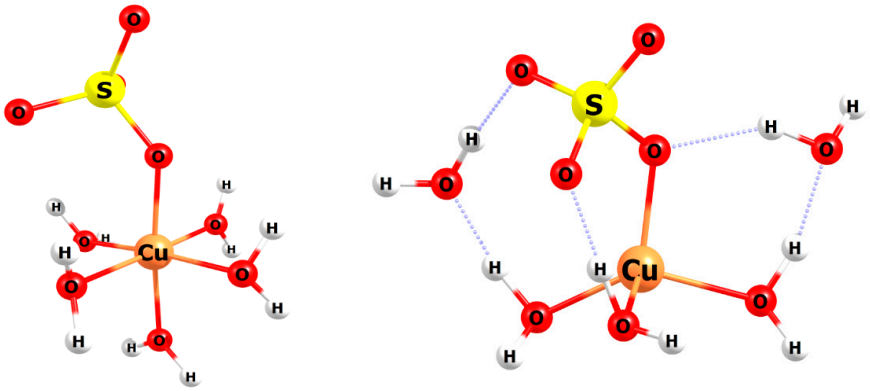

(**a**) (**b**)

Figure 7. Structures of the $CuSO_4 \cdot 5H_2O$ with the metal atom in the configuration: (**a**) octahedral; (**b**) tetrahedral.

The spatial structure of $CuSO_4 \cdot 5H_2O$ in interactions with the porous surface can be found, also, in a structure with the Cu atom in the tetrahedral configuration and with hydrogen-bonding interactions type with two water molecules (Figure 7b). In the octahedral configuration of the crystalline structure, the distance Cu-O is 1.83 Å. This value increases slightly for Cu-O-S to about 1.9 Å and just over 2 Å for Cu-O (H_2O) in the tetrahedral structure. When the cupric structure approaches the surface, an edge or a peak of the porous structure, the water of crystallization will be gradually removed and may leave the area of interest or may still be found around the active center by establishing hydrogen bonds. A direct interaction, a covalent bond, is thus formed between the Cu atom and an oxygen in the adsorbent medium, Si-O-Cu (Figure 8a), or Ti-O-Cu (Figure 8b). The distance between Cu atom and oxygen atom from the adsorbent decreases from 2 Å in crystalline structure to 1.9 Å.

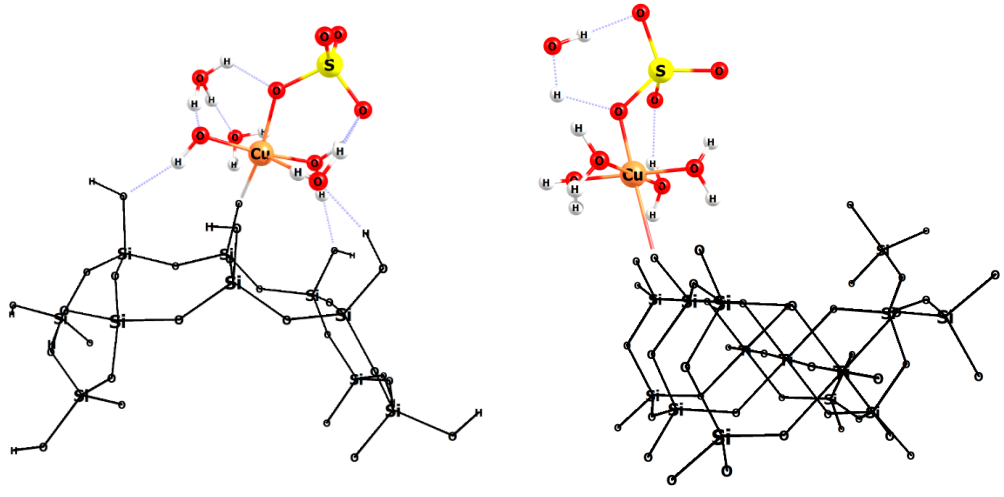

(**a**) (**b**)

Figure 8. The interaction of the structure $CuSO_4 \cdot 5H_2O$ with: (**a**) SBA-15, (**b**) ETS-10.

The removal of some crystallization water molecules and interactions with adsorbent structure determine the square plan hybridization (Figure 9a) or a pyramidal configuration (Figure 9b) for Cu atom, and formation of two covalent bonds with oxygen atom from the porous structures.

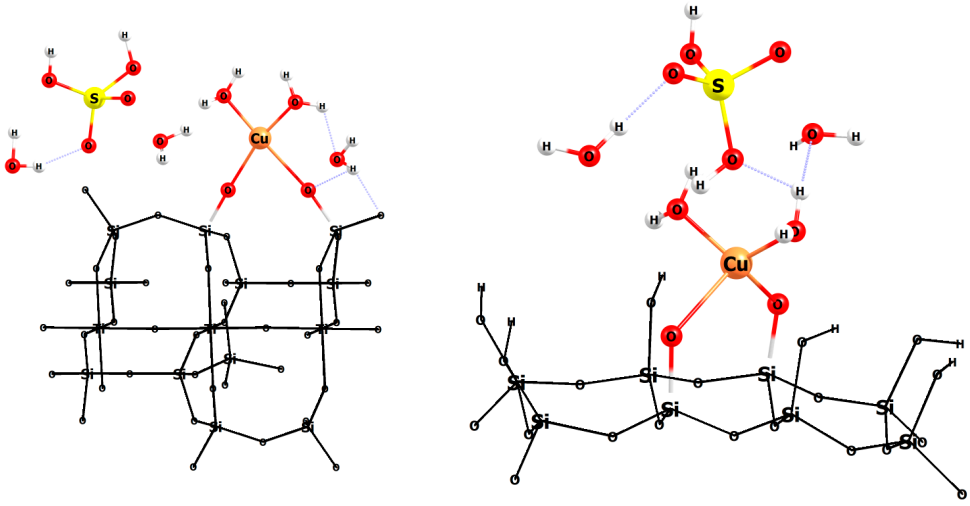

(**a**) (**b**)

Figure 9. The configuration of Cu atom in interactions with porous surface: (**a**) square planar; (**b**) tetrahedral.

In an acid environment, the sulfate fragment can form H_2SO_4, which is found in the system under investigation (Figure 8a).

4. Regeneration and Reusability of Sorbents

The applicability of potential sorbents depends on their regeneration under convenient conditions and the possibility of their re-use in successive sorption/desorption cycles. From practical motives, an ideal adsorbent must be reused in successive sorption/desorption cycles with as less as possible loss of the initial adsorption capacity. Therefore, desorption of Cu(II) ions was carried out in batch system by using the adsorbents loaded with copper immediately after the adsorption experiments. As eluent, 0.01 M solution of HCl in five successive sorption/desorption cycles was used and the obtained results are shown in Figure 10.

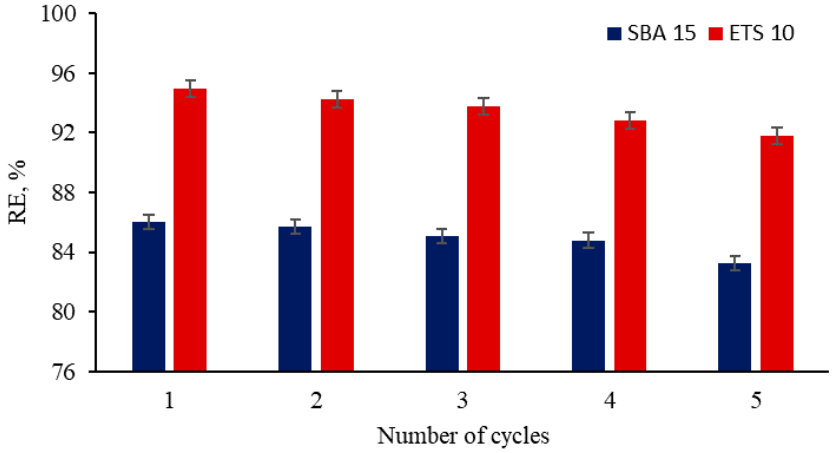

Figure 10. Reusability of the adsorbents under consecutive cycles sorption/desorption.

As can be seen, the removal efficiency slowly decreased during the sorption/desorption cycles, being about 91.75% for ETS-10, and 83.27% for SBA-15, respectively. These values recommend these materials as potential sorbents for efficient removal of Cu(II) from residual waters.

5. Conclusions

The sorption of Cu(II) ions from synthetic wastewaters onto titanosilicate ETS-10 and silica SBA-15 has been studied as a function of contact time, the initial metal ion concentration, adsorbent mass, pH, sorbent dose and temperature. Equilibrium, kinetic and thermodynamic data were applied in order to evaluate the efficiency of the investigated adsorbents for the removal of Cu(II) ions from aqueous solutions. The adsorption of Cu(II) on analyzed adsorbents obeyed the pseudo-second-order kinetics, supporting that the chemisorption would be the rate-determining step. The equilibrium data obtained for the adsorption of copper ions onto investigated adsorbents well fitted the Langmuir model with a maximum theoretical adsorption capacity of 52.71 mg Cu(II)/g for mesoporous silica SBA-15, and 172.53 mg Cu(II)/g for titanosilicate ETS-10, respectively. The adsorption process is endothermic ($\Delta H^\circ > 20$ kJ/mol) and spontaneous (the increase of the negative values of ΔG° with the increase of temperature). The adsorption of Cu(II) on the analyzed sorbents is a reversible process and the adsorbents can be used in five desorption/sorption cycles without significant loss in their adsorption capacities.

Experimental results showed that mesoporous silica SBA-15 and titanosilicate ETS-10 are promising adsorbents for the removal of copper ions from aqueous solutions.

Author Contributions: Conceptualization, I.Z., D.H. and N.Y.; methodology, I.Z., D.H., N.Y., D.G., M.I. and I.H.; software, D.G.; validation, D.G., I.Z. and D.H.; formal analysis, I.Z., D.H. and N.Y.; investigation, I.Z., D.H., N.Y., D.G., M.I. and I.H.; writing—original draft preparation, D.H., I.Z.; writing—review and editing, all authors; project administration, I.Z. and D.H.; funding acquisition, I.Z. and D.H. All authors have read and agreed to the published version of the manuscript.

Funding: This research was funded by IUCN-Dubna project No. 03-4-1128-2020/2022, theme 75. The APC was funded by the Alexandru Ioan Cuza University of Iasi research fund.

Institutional Review Board Statement: Not applicable.

Informed Consent Statement: Not applicable.

Data Availability Statement: The date presented in this study are available on the request from the corresponding author.

Acknowledgments: The authors are thankful to the Romanian Ministry of Research, Innovation and Digitization, within Program 1—Development of the national RD system, Subprogram1.2—Institutional Performance—RDI excellence funding projects, Contract No.11PFE/30.12.2021, for financial support.

Conflicts of Interest: The authors declare no conflict of interest.

References

1. Anastopoulos, I.; Massas, I.; Ehaliotis, C. Use of residues and by-products of the olive-oil production chain for the removal of pollutants from environmental media: A review of batch biosorption approaches. *J. Environ. Sci. Health Part A Toxic/Hazard. Subst. Environ. Eng.* **2015**, *50*, 677–718. [CrossRef] [PubMed]
2. González, A.G.; Pokrovsky, S.O.; Santana-Casiano, J.M.; González-Dávila, M. Bioadsorption of heavy metals. In *Prospects and Challenges in Algal Biotechnology*; Tripathi, B., Kumar, D., Eds.; Springer: Singapore, 2017; pp. 233–255. [CrossRef]
3. Peng, Q.; Liu, Y.; Zeng, G.; Xu, W.; Yang, C.; Zhang, J. Biosorption of copper(II) by immobilizing Saccharomyces cerevisiae on the surface of chitosan-coated magnetic nanoparticles from aqueous solution. *J. Hazard. Mater.* **2010**, *177*, 676–682. [CrossRef] [PubMed]
4. Ofomaja, A.E.; Naidoo, E.B.; Modise, S.J. Biosorption of copper(II) and lead(II) onto potassium hydroxide treated pine cone powder. *J. Environ. Manag.* **2010**, *91*, 1674. [CrossRef] [PubMed]
5. Moyo, M.; Chirinda, A.; Nharingo, T. Removal of copper from aqueous solution using chemically treated potato (*Solanum tuberosum*) leaf powder. *Clean Soil Air Water* **2016**, *44*, 488–495. [CrossRef]
6. Ekere, N.R.; Agwogie, A.B.; Ihedioha, J.N. Studies of biosorption of Pb^{2+}, Cd^{2+} and Cu^{2+} from aqueous solutions using Adansonia digitata root powders. *Int. J. Phytoremediat.* **2016**, *18*, 116–125. [CrossRef]
7. Chen, J.; Jiang, Y.; Shi, H.; Peng, Y.; Fan, X.; Li, C. The molecular mechanisms of copper metabolism and its roles in human diseases. *Pflügers Arch. Eur. J. Physiol.* **2020**, *472*, 1415–1429. [CrossRef]
8. Montazeri, A.; Akhlaghi, M.; Barahimi, A.R.; Jahanbazi Jahan Abad, A.; Jabbari, R. The Role of Metals in Neurodegenerative Diseases of the Central Nervous System. *Shefaye Khatam.* **2020**, *8*, 130–146. [CrossRef]

9. Mathys, Z.; White, A. Copper and Alzheimer's Disease. *Adv. Neurobiol.* **2017**, *18*, 199–216. [CrossRef]
10. Lundström, M.; Liipo, J.; Taskinen, P.; Aromaa, J. Copper precipitation during leaching of various copper sulfide concentrates with cupric chloride in acidic solutions. *Hydrometallurgy* **2016**, *166*, 136–142. [CrossRef]
11. Labidi, A.; Salaberria, A.M.; Fernandes, S.C.M.; Labidi, J.; Abderrabba, M. Adsorption of copper on chitin-based materials: Kinetic and thermodynamic studies. *J. Taiwan Inst. Chem. Eng.* **2016**, *65*, 140–148. [CrossRef]
12. Mushtaq, M.; Bhatti, H.N.; Iqbal, M.; Noreen, S. Eriobotrya japonica seed biocomposite efficiency for copper adsorption: Isotherms, kinetics, thermodynamic and desorption studies. *J. Environ. Manag.* **2016**, *176*, 21–33. [CrossRef]
13. Abdelfattah, I.; Ismail, A.A.; Sayed, F.A.; Almedolab, A.; Aboelghait, K.M. Biosorption of heavy metals ions in real industrial wastewater using peanut husk as efficient and cost effective adsorbent. *Environ. Nanotechnol. Monit. Manag.* **2016**, *6*, 176–183. [CrossRef]
14. Duan, H.; Wang, S.; Yang, X.; Yuan, X.; Zhang, Q.; Huang, Z.; Guo, H. Simultaneous separation of copper from nickel in ammoniacal solutions using supported liquid membrane containing synergistic mixture of M5640 and TRPO. *Chem. Eng. Res. Des.* **2017**, *117*, 460–471. [CrossRef]
15. Ntagia, E.; Rodenas, P.; Ter Heijne, A.; Buisman, C.J.N.; Sleutels, T.H.J.A. Hydrogen as electron donor for copper removal in bioelectrochemical systems. *Int. J. Hydrog. Energy* **2016**, *41*, 5758–5764. [CrossRef]
16. Ntimbani, R.N.; Simate, G.S.; Ndlovu, S. Removal of copper ions from dilute synthetic solution using staple ion exchange fibres: Dynamic studies. *J. Environ. Chem. Eng.* **2016**, *4*, 3143–3150. [CrossRef]
17. Lambert, A.; Drogui, P.; Daghrir, R.; Zaviska, F.; Benzaazoua, M. Removal of copper in leachate from mining residues using electrochemical technology. *J. Environ. Manag.* **2014**, *133*, 78–85. [CrossRef]
18. Ahluwalia, S.S.; Goyal, D. Removal of heavy metals by waste tea-leaves from aqueous solution. *Eng. Life Sci.* **2005**, *5*, 158–162. [CrossRef]
19. Awual, M.R.; Hasan, M.M.; Khaleque, M.A.; Sheikh, M.C. Treatment of copper(II) containing wastewater by a newly developed ligand based facial conjugate materials. *Chem. Eng. J.* **2016**, *288*, 368–376. [CrossRef]
20. Holub, M.; Balintova, M.; Kovacova, Z. Evaluation of Zeolite Adsorption Properties for Cu(II) Removal from Acidic Aqueous Solutions in Fixed-Bed Column System. *Proceedings* **2018**, *2*, 1293. [CrossRef]
21. Xiao, F.; Cheng, J.; Cao, W.; Yang, C.; Chen, J.; Luo, Z. Removal of heavy metals from aqueous solution using chitosan—Combined magnetic biochars. *J. Colloid. Interface. Sci.* **2019**, *540*, 579–584. [CrossRef]
22. Hussain, S.T.; Khaleefa Ali, S.A. Removal of heavy metal by ion exchange using bentonite clay. *J. Ecol. Eng.* **2021**, *22*, 104–111. [CrossRef]
23. Ali, I.; Burakov, A.E.; Melezhik, A.V.; Babkin, A.V.; Burakova, I.V.; Neskomornaya, M.E.A.; Galunin, E.V.; Tkachev, A.G.; Kuznetsov, D.V. Removal of Copper(II) and Zinc(II) Ions in Water on a Newly Synthesized Polyhydroquinone/Graphene Nanocomposite Material: Kinetics, Thermodynamics and Mechanism. *ChemistrySelect* **2019**, *4*, 12708–12718. [CrossRef]
24. Wang, Z.; Xu, W.; Jie, F.; Zhao, Z.; Zhou, K.; Liu, H. The selective adsorption performance and mechanism of multiwall magnetic carbon nanotubes for heavy metals in wastewater. *Sci. Rep.* **2021**, *11*, 16878. [CrossRef] [PubMed]
25. De Luca, P.; Bernaudo, I.; Elliani, R.; Tagarelli, A.; Nagy, J.; Macario, A. Industrial Waste Treatment by ETS-10 Ion Exchanger Material. *Materials* **2018**, *11*, 2316. [CrossRef]
26. Lv, L.; Su, F.; Zhao, X.S. Microporous titanosilicate ETS-10 for the removal of divalent heavy metals. *Stud. Surf. Sci. Catal.* **2005**, *156*, 933–940. [CrossRef]
27. De Luca, P.; Poulsen, T.G.; Salituro, A.; Tedeschi, A.; Vuono, D.; Kònya, Z.; Madaràsz, D.; Nagy, J.B. Evaluation and comparison of the ammonia adsorption capacity of titanosilicates ETS-4 and ETS-10 and aluminotitanosilicates ETAS-4 and ETAS-10. *J. Therm. Anal. Calorim.* **2015**, *122*, 1257–1267. [CrossRef]
28. De Luca, P.; Chiodo, A.; Nagy, J.B. Activated ceramic materials with deposition of photocatalytic titano-silicate micro-crystals. *Sustain. Chem.* **2011**, *154*, 155–165. [CrossRef]
29. Awual, M.R.; Rahman, I.M.M.; Yaita, T.; Khaleque, M.A.; Ferdows, M. pH dependent Cu(II) and Pd(II) ions detection and removal from aqueous media by an efficient mesoporous adsorbent. *Chem. Eng. J.* **2014**, *236*, 100–109. [CrossRef]
30. Zinicovscaia, I.; Yushin, N.; Humelnicu, D.; Grozdov, D.; Ignat, M.; Demcak, S.; Humelnicu, I. Sorption of Ce(III) by silica SBA-15 and titanosilicate ETS-10 from aqueous solution. *Water* **2021**, *13*, 3263. [CrossRef]
31. Langmuir, I. The adsorption of gases on plane surfaces of glass, mica and platinum. *J. Am. Chem. Soc.* **1918**, *143*, 1361–1403. [CrossRef]
32. Freundlich, H.M.F. Over the adsorption in solution. *J. Phys. Chem.* **1906**, *57*, 385–471.
33. Temkin, M. Adsorption equilibrium and the kinetics of processes on non-homogeneous surfaces and in the interaction between adsorbed molecules. *Zh. Fiz. Chim.* **1941**, *15*, 296–332.
34. Hall, K.R.; Eagleton, L.C.; Acrivos, A.; Vermeulen, T. Pore- and Solid-Diffusion Kinetics in Fixed-Bed Adsorption under Constant-Pattern Conditions. *Ind. Eng. Chem.* **1966**, *5*, 212–223. [CrossRef]
35. Ho, Y.S.; Huang, C.T.; Huang, H.W. Equilibrium sorption isotherm for metal ions on tree fern. *Process Biochem.* **2002**, *37*, 1421–1430. [CrossRef]
36. Keskinkan, O.; Göksu, M.Z.L.; Yüceer, A.; Basıbüyük, M.; Forster, C.F. Heavy metal adsorption characteristics of a submerged aquatic plant (*Myriophylum spicatum*). *Process Biochem.* **2003**, *39*, 179–183. [CrossRef]

37. Özer, A.; Özer, D.; Özer, A. The adsorption of copper(II) ions on to dehydrated wheat bran (DWB):determination of the equilibrium and thermodynamic parameters. *Process Biochem.* **2004**, *39*, 2183–2191. [CrossRef]
38. Liu, X.; Chen, Z.-Q.; Han, B.; Su, C.-L.; Han, Q.; Chen, W.-Z. Biosorption of copper ions from aqueous solution using rape straw powders: Optimization, equilibrium and kinetic studies. *Ecotoxicol. Environ. Saf.* **2018**, *150*, 251–259. [CrossRef]
39. Witek-Krowiak, A. Analysis of temperature-dependent biosorption of Cu^{2+} ions on sunflower hulls: Kinetics, equilibrium and mechanism of the process. *Chem. Eng. J.* **2012**, *192*, 13–20. [CrossRef]
40. Dinu, M.V.; Dinu, I.A.; Lazar, M.M.; Dragan, E.S. Chitosan-based ion-imprinted cryo-composites with excellent selectivity for copper ions. *Carbohydr. Polym.* **2018**, *186*, 140–149. [CrossRef]
41. Reddy, K.H.D.; Seshaiaha, K.; Reddy, A.V.R.; Lee, S.M. Optimization of Cd(II), Cu(II) and Ni(II) biosorption by chemically modified Moringa oleifera leaves powder. *Carbohydr. Polym.* **2012**, *88*, 1077–1086. [CrossRef]
42. Putra, W.P.; Kamari, A.; Yusoff, S.N.M.; Fauziah Ishak, C.; Mohamed, A.; Hashim, N.; Md Isa, I. Biosorption of Cu(II), Pb(II) and Zn(II) Ions from Aqueous Solutions Using Selected Waste Materials: Adsorption and Characterisation Studies. *J. Encapsulation Adsorpt. Sci.* **2014**, *4*, 25–35. [CrossRef]
43. Bazargan-Lari, R.; Zafarani, H.R.; Bahrololoom, M.E.; Nemati, A. Removal of Cu(II) ions from aqueous solutions by low-cost natural hydroxyapatite/chitosan composite: Equilibrium, kinetic and thermodynamic studies. *J. Taiwan Inst. Chem. Eng.* **2014**, *45*, 1642–1648. [CrossRef]
44. Laus, R.; Costa, T.G.; Szpoganicz, B.; Favere, V.T. Adsorption and desorption of Cu(II), Cd(II) and Pb(II) ions using chitosan crosslinked with epichlorohydrin-triphosphate as the adsorbent. *J. Hazard. Mater.* **2010**, *183*, 233–241. [CrossRef]
45. Langergren, S. About the theory of so-called adsorption of soluble substance. *Kung. Sven. Veten Hand.* **1898**, *24*, 1–39.
46. Ho, Y.S.; Mckay, G. Pseudo-second order model for sorption processes. *Process Biochem.* **1999**, *34*, 451–465. [CrossRef]
47. Weber, W.J.; Morris, J.C. Kinetics of adsorption on carbon from solution. *ASCE Sanit. Eng. Div. J.* **1963**, *89*, 31–39. [CrossRef]
48. Juang, R.S.; Chen, M.L. Application of the Elovich equation to the kinetics of metal sorption with solvent-impregnated resins. *Ind. Eng. Chem. Res.* **1997**, *36*, 813–820. [CrossRef]
49. Guo, Z.; Liu, X.; Huang, H. Kinetics and thermodynamics of reserpine adsorption onto strong acidic cationic exchange fiber. *PLoS ONE* **2015**, *10*, e0138619. [CrossRef]
50. Kumar, A.; Rout, S.; Ghosh, M.; Singhal, R.K.; Ravi, P.M. Thermodynamic parameters of U (VI) sorption onto soils in aquatic systems. *SpringerPlus* **2013**, *2*, 530. [CrossRef]
51. Lütke, S.F.; Igansi, A.V.; Pegoraro, L.; Dotto, G.L.; Pinto, L.L.A.; Cadaval, T.R.S. Preparation of activated carbon from black wattle bark waste and its application for phenol adsorption. *J. Environ. Chem. Eng.* **2019**, *7*, 103396. [CrossRef]
52. Sundaram, C.S.; Viswanathan, N.; Meenakshi, S. Defluoridation chemistry of synthetic hydroxyapatite at nano scale: Equilibrium and kinetic studies. *J. Hazard. Mater.* **2008**, *155*, 206–215. [CrossRef] [PubMed]